Bioinformatics Analysis of Gene Expression Profiles of Immune-mediated Necrotizing Myopathy

Jiaying Shi
First Hospital of Shanxi Medical University
Shule Wang
First Hospital of Shanxi Medical University
Jingfei Zhang
First Hospital of Shanxi Medical University
Xueli Chang
First Hospital of Shanxi Medical University
Juan Wang
First Hospital of Shanxi Medical University
Jing Zhang
First Hospital of Shanxi Medical University
Junhong Guo
First Hospital of Shanxi Medical University
Wei Zhang (zolkswagen@126.com)
Department of Neurology, The First Hospital, Shanxi Medical University, Taiyuan 030000, P. R. China

Research

Keywords: Immune-mediated necrotizing myopathy, bioinformatics analysis, cancer-related pathways, skeletal muscle construction, immune response

Posted Date: January 8th, 2021

DOI: https://doi.org/10.21203/rs.3.rs-137686/v1

Abstract

Background: Immune-mediated necrotizing myopathy (IMNM) is a type of autoimmune myopathy with limited therapeutic measures. This study aims to elucidate the potential biomarkers and investigate the underlying mechanisms in IMNM.

Materials and Methods: Microarray datasets in GSE128470 and GSE39454 were obtained from the Gene Expression Omnibus. Differentially expressed genes (DEGs) were filtrated by limma package in R statistical software. Functional enrichment analyses were performed using DAVID online tools. STRING database was used to construct protein-protein interaction (PPI) networks. The module analysis and hub genes validation were performed using Cytoscape software.

Results: Integrated analysis of two databases revealed 160 co-expressed DEGs in IMNM, including 80 downregulated genes and 80 upregulated genes. GO enrichment analysis revealed that sarcomere is the most significantly enriched GO term within the DEGs. KEGG pathway enrichment analysis revealed significant enrichment pathways in cancer. A PPI network consisting of 115 nodes and 205 edges were constructed and top 20 hub genes were identified. Two key modules from the network were identified. Eight hub genes in module 1 (*MYH3*, *MYH7B*, *MYH8*, *MYL5*, *MYBPH*, *ACTC1*, *YNNT 2* and *MYOG*) are tightly associated with skeletal muscle construction. Seven hub genes in module 2 (*C1QA*, *TYROBP*, *MS4A6A*, *RNASE6*, *FCGR2A*, *FCER1G* and *LAPTM5*) mainly take part in immune response.

Conclusions: Our research indicated that cancer-related pathways, skeletal muscle construction pathways and immune-mediated pathways might participate in the development of IMNM. Identified hub genes may serve as potential biomarkers or targets for early diagnosis.

Background

Immune-mediated necrotizing myopathy (IMNM), also described as necrotizing autoimmune myopathy (NAM), is a rare type of idiopathic inflammatory myopathies characterized by symmetric weakness of proximal limb muscle, high level of serum creatine kinase, infrequent extra-muscular involvement, along with distinctive histopathological characteristics including marked myofiber necrosis and regeneration with a lack of lymphocytic infiltrate [1]. The prevalence of IMNM is estimated to be around 10 cases per 100,000 people [2, 3]. IMNM is divided into three subtypes by serology markers: anti-signal recognition particle (anti-SRP) IMNM, anti-3-hydroxy-3-methylglutaryl–CoA reductase (anti-HMGCR) IMNM, and autoantibody-negative IMNM [1]. To date, the causes and pathological mechanisms underlying IMNM are still poorly understood. Several different factors are thought to contribute to IMNM, indicating the heterogeneity of the etiology of this entity. Substantial evidence exists to support the association between IMNM and various risk factors, including statin exposure, viral infections such as hepatitis C and HIV, malignancy and connective tissue diseases. Furthermore, a genetic component with strong immunogenetic predisposing factors has been postulated to predispose individuals to IMNM in the human leukocyte antigen (HLA)–DRB1 genotyping studies [4]. No random clinical trials exist to guide

treatment strategies in IMNM with the majority of the recommendations based on case series, longitudinal cohort studies, and experts' recommendation. It is agreed that treatment of IMNM ought to be initiated early and individualized to prevent long-term disability or recurrence [1]. However, treatment options of IMNM are still scarce and controversial. In the era of molecular-targeting drugs, it seems of utmost importance to explore its molecular mechanisms for the improvement of the diagnostic and therapeutic effects of IMNM.

Bioinformatics methods have been extensively used in medical oncology to evaluate the molecular mechanism in different types of human carcinogenesis. This study aims to identify the key genes and pathways that may be involved in the underlying pathomechanism of IMNM, narrow the target range and provide target therapy directions for further research using bioinformatics methods. Two original microarray datasets, GSE128470 and GSE39454 were acquired from the Gene Expression Omnibus (GEO) databases. Screening of differentially expressed genes (DEGs) were conducted followed by functional enrichment analysis. Protein-protein interaction (PPI) networks were established to select hub genes. Our results demonstrated that identified hub genes may serve as potential prognostic biomarkers in IMNM and pathways in cancer, skeletal muscle construction and immune response facilitate the understanding of the pathogenesis in IMNM.

Materials And Methods

Microarray Data

The raw gene expression profiles of GSE128470 and GSE39454 were acquired from the Gene Expression Omnibus database (https://www.ncbi.nlm.nih.gov/geo/) by searching the following key terms: ("necrotizing myopathy" OR "immune-mediated necrotizing myopathy" OR "necrotizing autoimmune myopathy"). GSE128470 was sequenced on the platform GPL96 (HG-U133A; Affymetrix Human Genome U133A Array) and GSE39454 was sequenced on the platform of the GPL570 (HG-U133_Plus_2; Affymetrix Human Genome U133 Plus 2.0 Array). Table 1 illustrated the information of the datasets.

Table 1
Basic information of the two microarray databases derived from the GEO database

Dataset ID	Subjects	Organization	Country	Number of samples (NM/NL)
GSE128470	Skeletal muscle	Brigham and Women's Hospital	United States	6/12
GSE39454	Skeletal muscle	MedImmune	United States	5/5

NM, necrotizing myopathy; NL, normal samples.

Data processing and differential expression analysis

The data processing was performed utilizing the R statistical software (version 4.0.1; https://www.r-project.org/) and Bioconductor analysis tools (http://www.bioconductor.org/). The original files were transformed to probelevel data and converted into an international standard name for genes (gene-symbol). Probe sets without corresponding gene symbols were removed. If several probe symbols mapped to one particular gene, the mean of the probes was calculated as the final gene expression value. Screening of DEGs between necrotizing myopathy (NM) samples and normal (NL) samples was conducted using the limma package in R after background correction and quantile normalization. Only genes differentially expressed with a Pvalue < 0.05 were selected and saved in CSV files for further analyses. Subsequently, DEGs were identified with the cutoff criteria of an absolute log fold-change (FC) value (|log2FC|) > 1 in GSE128470 and |log2FC|>0.653 in GSE39454 so as to get sufficient co-expressed DEGs in both datasets for further enrichment analysis.

Volcano plots were generated to present all the up- and down-regulated DEGs for visualization. To test the predictive value of the identified DEGs, hierarchical clustering analysis was conducted separately for all samples in the two datasets using the pheatmap package in R (The R Foundation; https://cran.rproject.org/web/packages/pheatmap/index.html). Venn diagram displayed the overlapped DEGs between the two profiles with the up-regulated genes and down-regulated genes intersected respectively. The top 100 overlapped DEGs were displayed by heatmap visualization.

GO and KEGG pathway analysis of DEGs

Gene Ontology (GO; http://www.geneontology.org/) and the Kyoto Encyclopedia of Genes and Genomes (KEGG; http://www.genome.jp/kegg/) pathway enrichment analyses were implemented to analyze the biological characteristics of the identified DEGs via the Database for Annotation, Visualization and Integrated Discovery (DAVID;version 6.8; https://david.ncifcrf.gov/) online tools [5]. The GO analysis classifies functions along three categories: molecular function, biological process, and cellular component. The signaling pathway with a P-value < 0.05 was considered significant in statistics. Bubble diagrams were used to show the results of the GO terms and KEGG pathway enrichment analyses of the overlapping DEGs.

PPI network construction and hub genes identification

The Search Tool for the Retrieval of Interacting Genes [6] (STRING, version 11.0; https://string-db.org/) is a pre-computed global resource for demonstrating the interaction information derived from predictions and experiments. In the current study, we constructed PPI networks of the overlapped DEGs utilizing the STRING database with a confidence score of ≥ 0.4 for significant differences. Cytoscape software (version 3.6.1, http://www.cytoscape.org/), a platform for visualizing complex networks and integrating these with any type of attribute data, was implemented to establish a PPI network, in which nodes represent proteins and edges represent the relationship of proteins. The connectivity degree was statistically analyzed by their combined scores based on the database algorithms. The highly connected nodes in the network were identified and labeled as hub genes utilizing the cytoHubba tool kits of the Cytoscape. The MCODE plug-in was applied to quantify the degree of each protein node and explore

significant modules. MCODE scores > 5, degree cut-off = 2, node score cut-off = 0.2, Max depth = 100 and k-score = 2 were defined as the threshold values.

Results

Heterogeneity Test and Preliminary Screening of DEGs

All data were illustrated by box plots. As shown in Fig. 1, the median of NM and NL samples was almost on the same line, indicating superior effectiveness of standardization. Volcano Plots were applied to visualize the DEGs, in which red dots represent the upregulated genes and blue dots represent the downregulated genes. A total of 1070 DEGs (526 upregulated and 543 downregulated genes) in GSE128470 and 704 DEGs (453 upregulated and 251 downregulated genes) in GSE39454 were identified according to the cut-off criteria described above (Fig. 2). Hierarchical clustering analysis was carried out separately for all samples in the two cohorts according to the overlapped DEGs, revealing that the patients were clearly separated into two clusters based on the expression levels of the identified DEGs (Fig. 3). The consistently up- and downregulated genes in both cohorts were selected and presented using Venn diagram. 160 significant co-expressed DEGs were finally confirmed, including 80 downregulated DEGs and 80 upregulated DEGs (Fig. 4). The top 100 co-expressed DEGs were displayed by heatmap visualization in Fig. 5, which also revealed that the DEGs expression patterns varied between the NM and NL groups.

Functional enrichment analysis

In order to better look into the biological functions of the DEGs in IMNM, the overall 160 DEGs were predicted by DAVID for further analysis. A total of 94 GO terms were associated with the DEGs with 21 significantly enriched GO terms that met the cut-off criteria of P-value < 0.05. The top ten significantly enriched terms in biological process, cellular component and molecular function were shown in Fig. 6. In biological process term, we found that the DEGs were mainly abundant in regulation of transcription (DNA-templated), ossification, muscle filament sliding, insulin-like growth factor receptor signaling pathway and skeletal muscle contraction (Fig. 6A). In molecular function term, the DEGs were mostly enriched in protein binding, identical protein binding, calcium ion binding, protein homodimerization activity and calmodulin binding (Fig. 6B). In cellular component term, the DEGs were predominantly involved in extracellular exosome, cytosol, membrane raft, lysosome, sarcomere and myosin filament (Fig. 6C). KEGG pathway analysis presented that adrenergic signaling in cardiomyocytes, pathways in cancer, small cell lung cancer, ECM-receptor interaction, tryptophan metabolism, focal adhesion, oxytocin signaling pathway and cGMP-PKG signaling pathway were most highly related (Fig. 6D).

PPI network and module analysis

A PPI network consisting of 115 nodes and 205 edges was constructed, setting $P < 0.05$, coefficients of $|r| > 0.4$ as a strict threshold. Figure 7 illustrated the co-expression network performed by Cytoscape,

displaying the interactions of the overlapping DEGs. Then, by using the MCODE plug-in, we identified two key modules from the PPI network (Fig. 8). The module 1, which exhibited the highest score, consisted of 8 nodes (i.e. *MYH3*, *MYH7E*, *MYH8*, *MYL5*, *MYBPH*, *ACTC1*, *YNNT 2* and *MYOG*) and 25 edges. The module 2 containing 7 nodes (i.e. *C1QA*, *TYROBP*, *MS4A6A*, *RNASE6*, *FCGR2A*, *FCER1G* and *LAPTM5*) and 20 edges, also possessed a strong connection. These findings implied that the afore-mentioned genes with higher hub degrees tend to exert a potential influence in IMNM.

Identification of hub genes

Hub genes from the whole network were extracted using the plug in cytoHubba application. Top 20 hub genes were selected based on multiform algorithm (i.e. MCC, MNC, DMNC and Degree) as shown in Table 2. They are *ACTC1, MYH3, MYH8, MYH7B, C1QA, FCER1G, TYROBP, TNNT2, MYL5, LAPTM5, MS4A6A, FCGR2A, MYOG, RNASE6, MYBPH, FN1, CXCR4, SPP1, ESR1* and *CD24.* The interactions among them are shown in Fig. 9.

Table 2
The statistical results of the connectivity of the network

Gene	MCC	MNC	DMNC	Degree
ACTC1	363	8	0.55399	9
MYH3	362	8	0.55398	8
MYH8	360	7	0.65858	7
MYH7B	360	7	0.65858	7
C1QA	248	7	0.58540	9
FCER1G	246	7	0.58540	7
TYROBP	244	8	0.46651	8
TNNT2	242	7	0.54881	7
MYL5	242	7	0.54881	7
LAPTM5	241	6	0.66569	7
MS4A6A	240	6	0.66570	6
FCGR2A	132	6	0.57059	9
MYOG	124	5	0.64826	9
RNASE6	122	6	0.52304	6
MYBPH	121	5	0.64826	6
FN1	61	15	0.22033	20
CXCR4	42	9	0.33413	13
SPP1	34	8	0.37904	8
ESR1	32	9	0.23866	18
CD24	23	6	0.38039	9

Discussion

IMNM is a subtype of idiopathic inflammatory myopathies associated with different environmental and genetic and cancer risks factors. Despite opportune immunosuppressant treatment, a majority of IMNM patients still suffer from persistent and significant weakness with a relatively poorer prognosis compared with other types of myositis [7–9]. Therefore, comprehending the genetic mechanisms and discovering novel molecular targets are crucial for improving the therapeutic effects. This study analyzed gene expression profiles, identified IMNM-related DEGs and enabled identification of potential candidate genes

and pathways, aiming at investigating the pathogenesis of IMNM at the genome level and finding target therapy directions.

After screening differentially expressed genes, 160 significant co-expressed DEGs in two databases were identified, including 80 downregulated DEGs and 80 upregulated DEGs. GO enrichment analysis revealed that sarcomere is the most significantly enriched GO term within the DEGs. Muscle contraction is controlled by a family of sarcomeric myosin motors, which consist of myosin heavy chains and myosin light chains. Proximal muscle weakness is the typical clinical characteristics of IMNM patients, suggesting the destruction of the muscle's essential contractile machinery. Therefore, it is hypothesized that the immune-induced destruction of chemo-mechanical properties of the myosin motors may be potentially critical in the pathological mechanism of IMNM. However, whether or not the muscle weakness in IMNM patients is caused by impairment of sarcomere dynamics remains to be fully clarified.

KEGG pathway enrichment analysis focused on eight significant pathways, of which small cell lung cancer, ECM-receptor interaction and focal adhesion fall within cancer-related pathways. ECM-receptor interaction pathway is crucially important in the process of tumor shedding, adhesion, degradation, movement and hyperplasia. The function of ECM has been verified in various cancers such as prostate [10], gastric [11] and breast cancer [12], etc. Focal adhesion signaling hubs critically regulated cell behavior, impacted on tumor cell survival and served as potential cancer targets [13]. Notably, cancer can be diagnosed prior to, concurrent with, or after the diagnosis of IMNM, suggesting that the two courses might be closely related [14, 15]. A pronounced higher risk of cancer has been demonstrated in HMGCR-positive IMNM [16] in line with previous data showing a trend towards increased incidence of cancer in IMNM [17]. Consequently, it’s tempting to speculate that the anti-tumor immune response may act as a key process in the pathogenesis of IMNM, as recently outlined in other autoimmune settings [14]. Several lines of evidence support the hypothesis that a cancer-associated autoimmune mechanism might participate in the process of idiopathic inflammatory myopathies [15]. One possible mechanism is that mutant proteins in tumors may become the target of an antitumor response which could be redirected to the wild-type proteins, ultimately resulting in damage to normal healthy tissues [15]. Another possible mechanism is that the overexpression of an autoantigen by tumor cells leads to abnormal processing or cleavage of the protein, generating cryptic epitopes not previously encountered by the immune system, initiating autoimmunity and damaging muscle and other target tissues [15]. Our results provided additional evidence for the potential association between IMNM and cancer.

We afterwards constructed a PPI network consisting of 115 nodes and 205 edges. Since modules with more complex interactions tend to exhibit more critical roles in the underlying mechanisms, two significant modules in PPI network were identified and taken into further analysis. Notably, all 15 genes identified in module analysis were simultaneously hub genes, indicating that these genes might be crucial in the development of IMNM. Eight hub genes in module 1 (*MYH3, MYH7B, MYH8, MYL5, MYBPH, ACTC1, YNNT 2* and *MYOG*) are tightly associated with skeletal muscle construction. Seven hub genes in module 2 (*C1QA, TYROBP, MS4A6A, RNASE6, FCGR2A, FCER1G* and *LAPTM5*) mainly take part in

immune response. Interaction network for the top 20 hub genes supports the distribution of these two pathways as well.

Eight hub genes identified in module 1 encode proteins that are either a muscle-specific transcription factor that can induce myogenesis, namely *MYOG*, or components of the skeletal muscle sarcomeric filament, including *MYH3, MYH8, MYH7B, TNNT2, MYL5, MYBPH* and *ACTC1*. Mechanistically, myogenin binds to the myomaker promoter, regulates myocyte fusion, and is required for expression of myomaker [18]. Given that the prominent fiber necrosis and regeneration are the pathological characteristics of IMNM, we proposed *MYOG* as a regulator of the enhanced regenerative responses in muscle homeostasis. The molecular changes underlying muscle weakness remain unclear in IMNM. Lassche *et.al* conducted an experiment on contractile function in IBM and found that the reduced formation of attached actin-myosin cross-bridges may lead to muscle fiber weakness [19]. A study on nemaline myopathy with definite mutations also revealed impaired actin-myosin interaction causing decreased muscle fiber force [20]. Therefore, our findings suggest that the dysregulation of these genes associated with skeletal muscle construction are likely to be pathogenic in IMNM. The contractile function in IMNM have not been studied yet. Further researches are desperately needed for verification.

Evidence exists to support the strong immunogenetic predisposing factors contributing to IMNM [4, 21, 22]. Seven hub genes identified in module 2 are strongly linked to immune response, including *C1QA, TYROBP, MS4A6A, RNASE6, FCGR2A, FCER1G* and *LAPTM5*. The functions of these genes in immune system were listed in Table 3. Notably, *C1QA* is a component of calcium-dependent complex of the 3 subcomponents C1q, which was observed at the sarcolemmal level in IMNM patients, suggesting classical pathway activation (antibody-dependent) of complement [23]. In IMNM, the identification of a significant amount of CD4 + and CD8 + T cells, grouped in the endomysial and perimysial compartment, and a strong and ubiquitous up-regulation of MHC class I major histocompatibility complex on the sarcolemma and MAC deposition on endomysial capillaries strongly support the involvement of an immune-mediated process [24]. Allenbach *et. al* showed that sarcolemmal C5b-9 deposits correlated with necrosis and that the classical complement pathway was activated [23]. Evidence demonstrated that IMNM is essentially a Th1-M1–mediated disease in which high levels of IFN-γ, TNF-α, IL-12, and STAT1 functionally regulate the immune response [24]. However, the underlying immune response in IMNM still needs to be addressed in detail. Even if our findings are not contributing directly or indirectly to the disease pathology, they nonetheless provide evidence in an accessible manner of a mechanism likely to be occurring in IMNM, which may guide a direction for future work. Discovery of these genes and identification of their roles in IMNM may offer useful information regarding the treatment of IMNM.

Table 3
Hub genes strongly linked to immune response in module 2.

Gene	Functions in immune response
C1QA	C1QA, the initiator of the complement classical pathway, restrains the response to self-antigens by modulating the mitochondrial metabolism of CD8 + T cells, which can themselves propagate autoimmunity [25].
FCER1G	FCER1G, the high-affinity IgE receptor, participates in the process of immune cell infiltration [26].
LAPTM5	LAPTM5, encoding a membrane protein that localizes to intracellular vesicles, is essential for the lysosomal degradation of T cell and B cell antigen receptors through the transport endosomes to lysosomes [27].
TYROBP	TYROBP associates with activating receptors recognizing major histocompatibility complex (MHC) class III molecules on the plasma membrane of NK cells.
MS4A6A	MS4A6A expression predominates in classical monocytes (M0) and their M2 derivatives.
RNASE6	RNASE6 belongs to the ribonuclease A (RNaseA) superfamily and is secreted by innate immune cells with anti-infective and immune-regulatory properties [28].
FCGR2A	FCGR2A (CD32), a receptor for the Fc portion of IgG, participates in diverse immunomodulatory functions such as phagocytosis of immune complexes and modulation of antibody production by B cells [29].

Conclusions

Taken together, the results of the bioinformatics analysis of two GEO microarray datasets of IMNM indicated that cancer-related pathways, skeletal muscle construction pathways and immune-mediated pathways probably participate in the development of IMNM. The discovery of hub genes that are implicated in IMNM was an impetus to unravel the pathophysiology of this debilitating disease, including *MYH3, MYH7B, MYH8, MYL5, MYBPH, ACTC1, YNNT 2, MYOG, C1QA, TYROBP, MS4A6A, RNASE6, FCGR2A, FCER1G* and *LAPTM5*. Further studies need to be implemented to investigate the molecular mechanisms and biological functions of the hub genes and to estimate whether they can serve as novel potential biomarkers or therapeutic targets in IMNM patients.

Abbreviations

IMNM = Immune-mediated necrotizing myopathy; NAM = Necrotizing autoimmune myopathy; NM = Necrotizing myopathy; NL = Normal; GEO = Gene Expression Omnibus; DEGs = differentially expressed genes; GO = Gene Ontology; KEGG = Kyoto Encyclopedia of Genes and Genomes; PPI = protein-protein interaction; DAVID = Database for Annotation, Visualization and Integrated Discovery; STRING = The Search Tool for the Retrieval of Interacting Genes; anti-SRP = anti-signal recognition particle; anti-HMGCR = anti-3-hydroxy-3-methylglutaryl–CoA reductase; ACTC1 = Actin, alpha cardiac muscle 1; MYH3 = Myosin heavy chain 3; MYH8 = Myosin heavy chain 8; MYH7B = Myosin heavy chain 7B; C1QA = Complement C1q subcomponent subunit A; FCER1G = High affinity immunoglobulin epsilon receptor subunit gamma / Fc

receptor gamma-chain; TYROBP = TYRO protein tyrosine kinase-binding protein; TNNT2 = Troponin T, cardiac muscle; MYL5 = Myosin regulatory light chain 5; LAPTM5 = Lysosomal-associated transmembrane protein 5; MS4A6A = Membrane-spanning 4-domains subfamily A member 6A; FCGR2A = Low affinity immunoglobulin gamma Fc region receptor II-a / IgG Fc receptor II-a; MYOG = Myogenin; RNASE6 = Ribonuclease K6; MYBPH = Myosin-binding protein H; FN1 = Fibronectin; CXCR4 = C-X-C chemokine receptor type 4; SPP1 = Sphingosine-1-phosphate phosphatase 1; ESR1 = Estrogen receptor and CD24 = Signal transducer CD24.

Declarations

Availability of data and materials

The datasets used and/or analyzed during the current study are available from the corresponding author on reasonable request.

Competing interest

The authors declare that they have no competing interests.

Funding

Funding information is not applicable.

Authors' contributions

JS and SW performed data analyses and wrote the manuscript. JZ, JW, XC and JZ contributed significantly to data interpretation and manuscript revision. JS, SW, WZ and JG conceived and designed the study. All authors read and approved the final version of the manuscript.

Acknowledgements

Not applicable.

References

1. Pinal-Fernandez I, Casal-Dominguez M, Mammen AL. Immune-Mediated Necrotizing Myopathy. Curr Rheumatol Rep, 2018; 20: 21
2. Dobloug C, Garen T, Bitter H et al. Prevalence and clinical characteristics of adult polymyositis and dermatomyositis; data from a large and unselected Norwegian cohort. Ann Rheum Dis, 2015; 74: 1551-1556
3. Svensson J, Arkema EV, Lundberg IE, Holmqvist M. Incidence and prevalence of idiopathic inflammatory myopathies in Sweden: a nationwide population-based study. Rheumatology (Oxford), 2017; 56: 802-810

4. Ohnuki Y, Suzuki S, Shiina T et al. HLA-DRB1 alleles in immune-mediated necrotizing myopathy. Neurology, 2016; 87: 1954-1955.
5. Huang da W, Sherman Bt Fau - Lempicki RA, Lempicki RA. Systematic and integrative analysis of large gene lists using DAVID bioinformatics resources. Nat. Protoc, 2009; 4: 44-57
6. Szklarczyk D, Franceschini A, Wyder S et al. STRING v10: protein-protein interaction networks, integrated over the tree of life. Nucleic acids research, 2015; 43: D447-452
7. Suzuki S, Nishikawa A, Kuwana M et al. Inflammatory myopathy with anti-signal recognition particle antibodies: case series of 100 patients. Orphanet J Rare Dis, 2015; 10: 61
8. Pinal-Fernandez I, Parks C, Werner JL et al. Longitudinal Course of Disease in a Large Cohort of Myositis Patients With Autoantibodies Recognizing the Signal Recognition Particle. Arthritis Care Res (Hoboken), 2017; 69: 263-270
9. Tiniakou E, Pinal-Fernandez I, Lloyd TE et al. More severe disease and slower recovery in younger patients with anti-3-hydroxy-3-methylglutaryl-coenzyme A reductase-associated autoimmune myopathy. Rheumatology (Oxford), 2017; 56: 787-794
10. Andersen MK, Rise K, Giskeodegard GF et al. Integrative metabolic and transcriptomic profiling of prostate cancer tissue containing reactive stroma. Sci Rep, 2018; 8: 14269
11. Yan P, He Y, Xie K, Kong S, Zhao W. In silico analyses for potential key genes associated with gastric cancer. PeerJ, 2018; 6: e6092
12. Bao Y, Wang L, Shi L et al. Transcriptome profiling revealed multiple genes and ECM-receptor interaction pathways that may be associated with breast cancer. Cell Mol Biol Lett, 2019
13. Eke I, Cordes N. Focal adhesion signaling and therapy resistance in cancer. Semin Cancer Biol, 2015; 31: 65-75
14. Joseph CG, Darrah E, Shah AA et al. Association of the autoimmune disease scleroderma with an immunologic response to cancer. Science, 2014; 343: 152-157
15. Tiniakou E, Mammen AL. Idiopathic Inflammatory Myopathies and Malignancy: a Comprehensive Review. Clin Rev Allergy Immunol, 2017; 52: 20-33
16. Allenbach Y, Keraen J, Bouvier AM et al. High risk of cancer in autoimmune necrotizing myopathies: usefulness of myositis specific antibody. Brain, 2016; 139: 2131-2135
17. Limaye V, Bundell C, Hollingsworth P et al. Clinical and genetic associations of autoantibodies to 3-hydroxy-3-methyl-glutaryl-coenzyme a reductase in patients with immune-mediated myositis and necrotizing myopathy.
18. Jones JM, Player DJ, Samanta S et al. Hyaluronan derived nanoparticle for simvastatin delivery: evaluation of simvastatin induced myotoxicity in tissue engineered skeletal muscle. Biomater Sci, 2019; 8: 302-312
19. Lassche S, Rietveld A, Heerschap A et al. Muscle fiber dysfunction contributes to weakness in inclusion body myositis. Neuromuscul Disord, 2019; 29: 468-476

20. de Winter Jm Fau - Ottenheijm CAC, Ottenheijm CAC. Sarcomere Dysfunction in Nemaline Myopathy. Neuromuscul Dis, 2017; 4: 99-113
21. Kishi T, Rider LG, Pak K et al. Association of Anti-3-Hydroxy-3-Methylglutaryl-Coenzyme A Reductase Autoantibodies With DRB1*07:01 and Severe Myositis in Juvenile Myositis Patients. Arthritis Care Res (Hoboken), 2017; 69: 1088-1094
22. Mohassel P, Foley AR, Donkervoort S et al. Anti-3-hydroxy-3-methylglutaryl-coenzyme a reductase necrotizing myopathy masquerading as a muscular dystrophy in a child. Muscle Nerve, 2017; 56: 1177-1181
23. Allenbach Y, Arouche-Delaperche L, Preusse C et al. Necrosis in anti-SRP(+) and anti-HMGCR(+)myopathies: Role of autoantibodies and complement. Neurology, 2018; 90: e507-e517
24. Preuße C, Goebel Hh Fau - Held J, Held J Fau - Wengert O et al. Immune-mediated necrotizing myopathy is characterized by a specific Th1-M1 polarized immune profile. American Journal of Pathology, 2012; 181: 2161-2171
25. Ling GS, Crawford G, Buang N et al. C1q restrains autoimmunity and viral infection by regulating CD8(+) T cell metabolism. Science, 2018; 360: 558-563
26. Zhang GA-O, Bogdanova N, Gao T, Sheikh KA. Elimination of activating Fcγ receptors in spontaneous autoimmune peripheral polyneuropathy model protects from neuropathic disease. PloS one, 2019; 14: e0220250
27. Ishihara T, Inoue J, Kozaki K, Imoto I, Inazawa J. HECT-type ubiquitin ligase ITCH targets lysosomal-associated protein multispanning transmembrane 5 (LAPTM5) and prevents LAPTM5-mediated cell death. The Journal of biological chemistry, 2011; 286: 44086-44094
28. Lu L, Arranz-Trullen J, Prats-Ejarque G, Pulido D, Bhakta S, Boix E. Human Antimicrobial RNases Inhibit Intracellular Bacterial Growth and Induce Autophagy in Mycobacteria-Infected Macrophages. Front Immunol, 2019; 10: 1500
29. Heitmann JA-O, Hagelstein I, Hinterleitner CA-O et al. Fc gamma receptor expression serves as prognostic and diagnostic factor in AML. Leukemia and Lymphoma, 2020; 5: 1-9

Figures

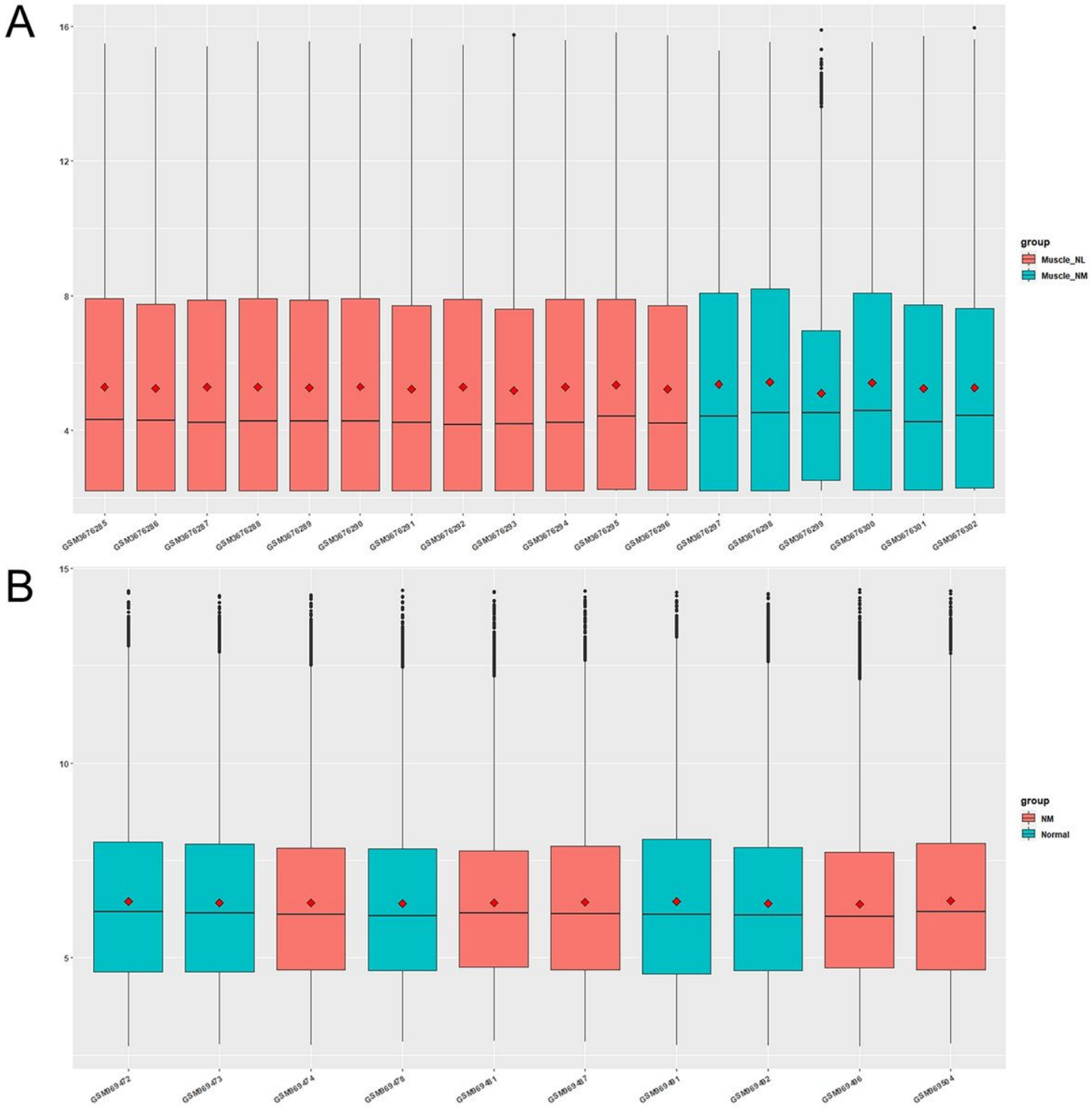

Figure 1

The box plots of gene expression level in two databases. (A) GSE128470; (B) GSE39454.

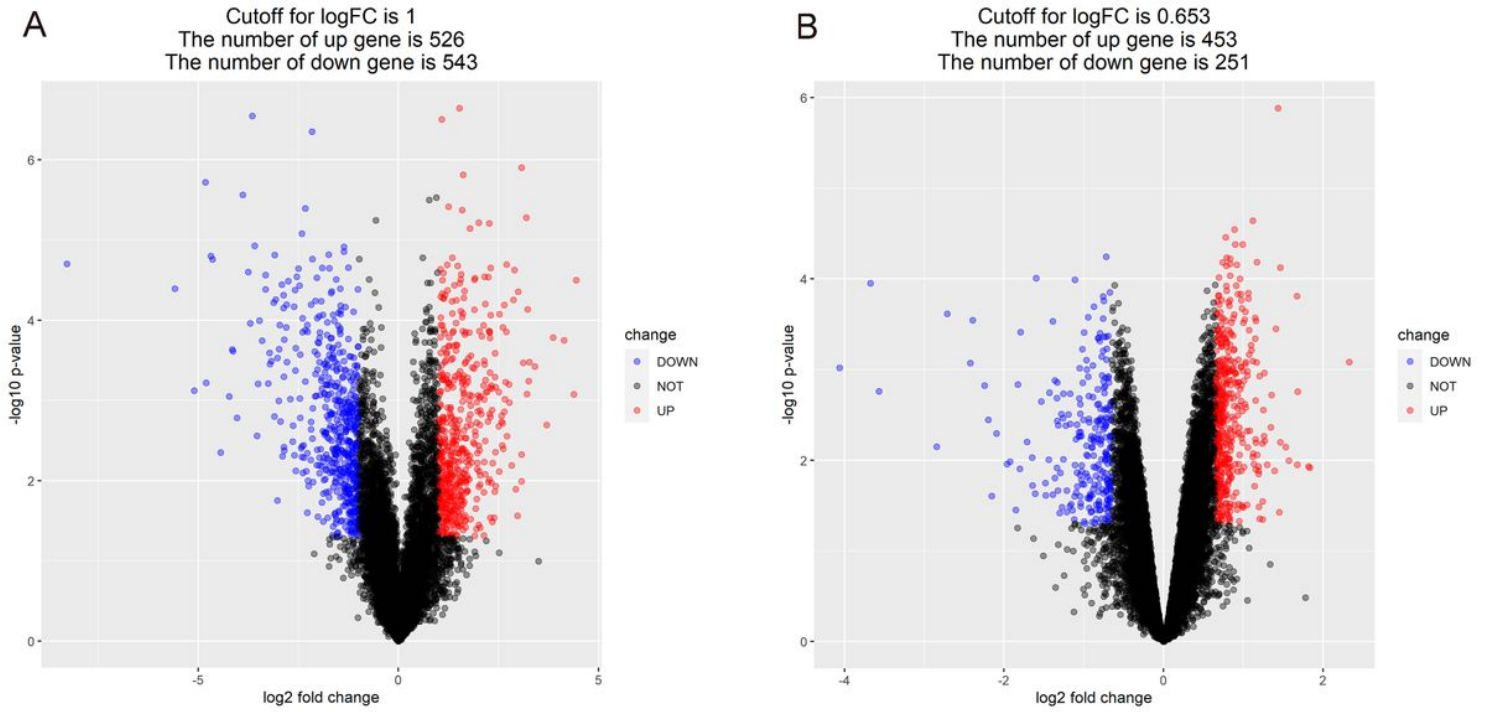

Figure 2

Volcano plots of DEGs in two databases. (A) Volcano plot of GSE128470; (B) Volcano plot of GSE39454. Abbreviations: NL, normal; NM: necrotizing myopathy

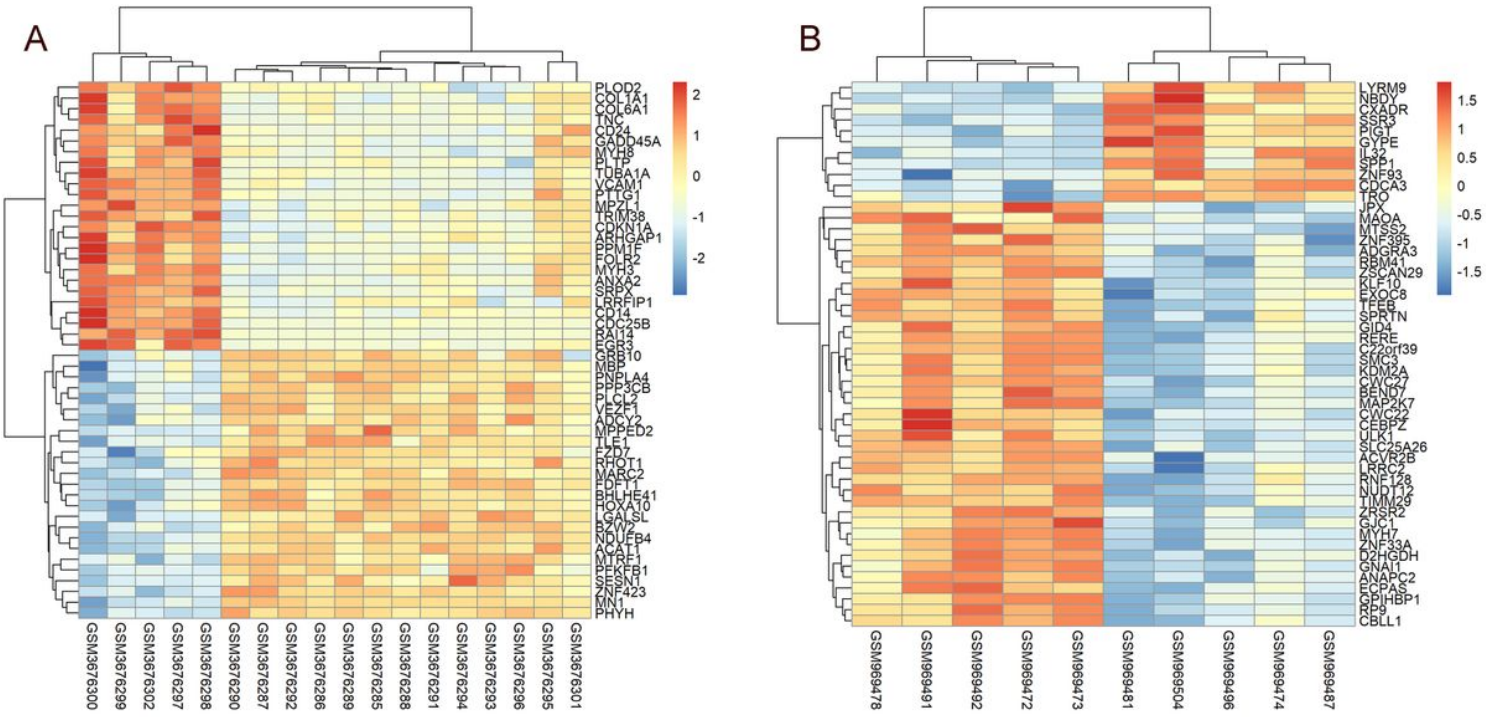

Figure 3

Heatmaps of DEGs in two databases. (A) Heatmap of GSE128470; (B) Heatmap of GSE39454. Abbreviations: DEGs, differentially expressed genes.

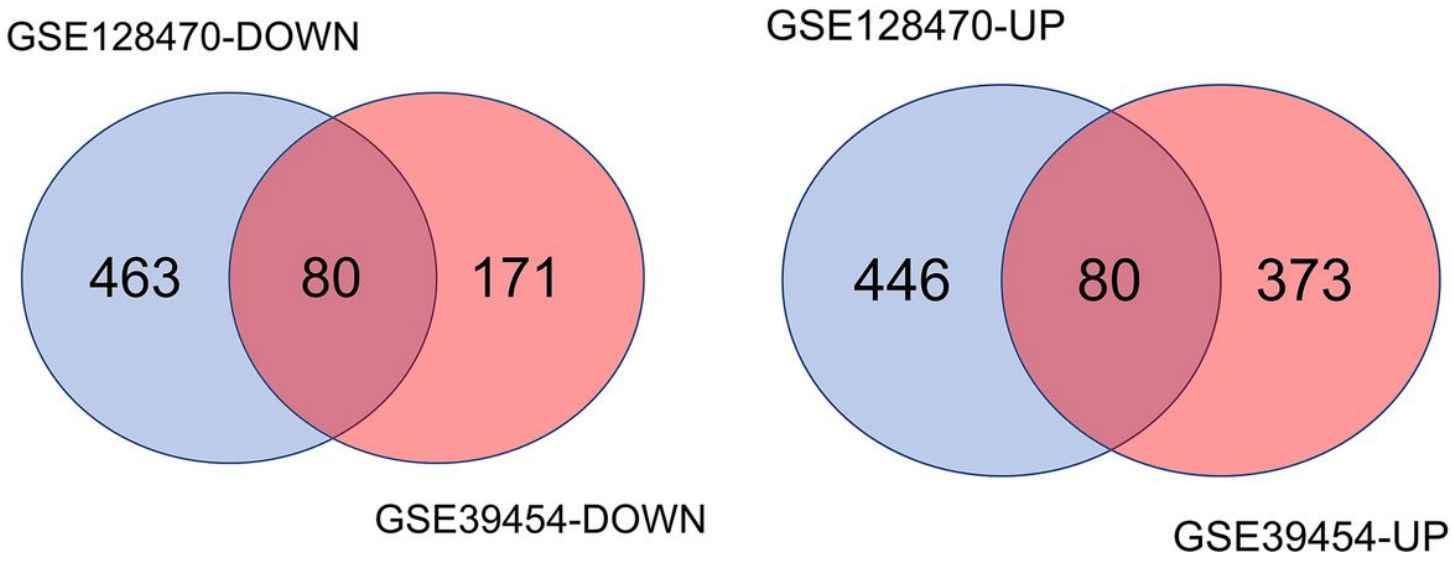

Figure 4

Venn diagrams of upregulated and downregulated overlapping DEGs. Abbreviations: DEGs, differentially expressed genes; GEO, Gene Expression Omnibus.

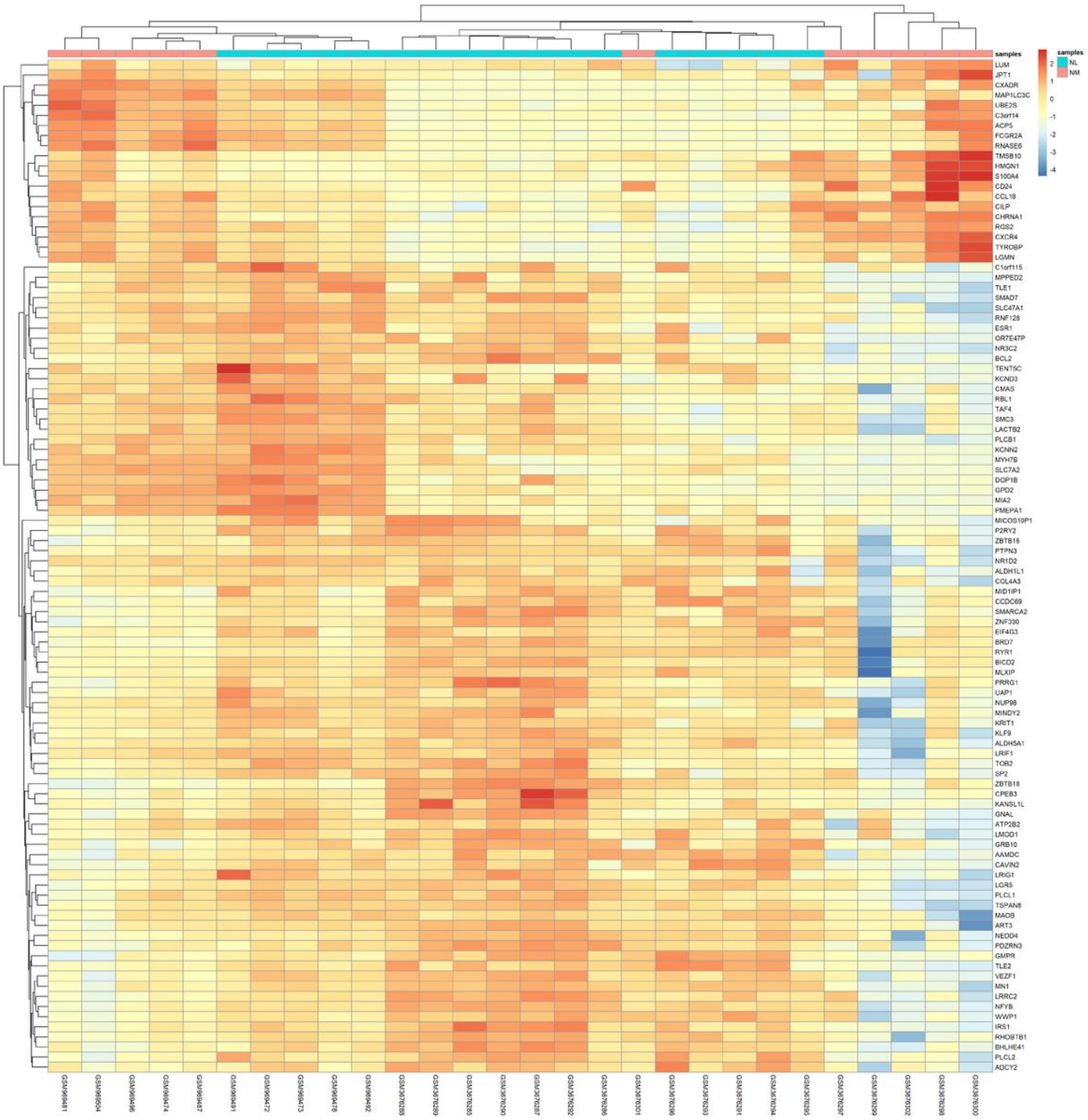

Figure 5

Hierarchical clustering heatmap of the top 100 overlapping DEGs. The color in the heatmap from blue to red shows the progression from low expression to high expression. Abbreviations: DEGs, differentially expressed genes.

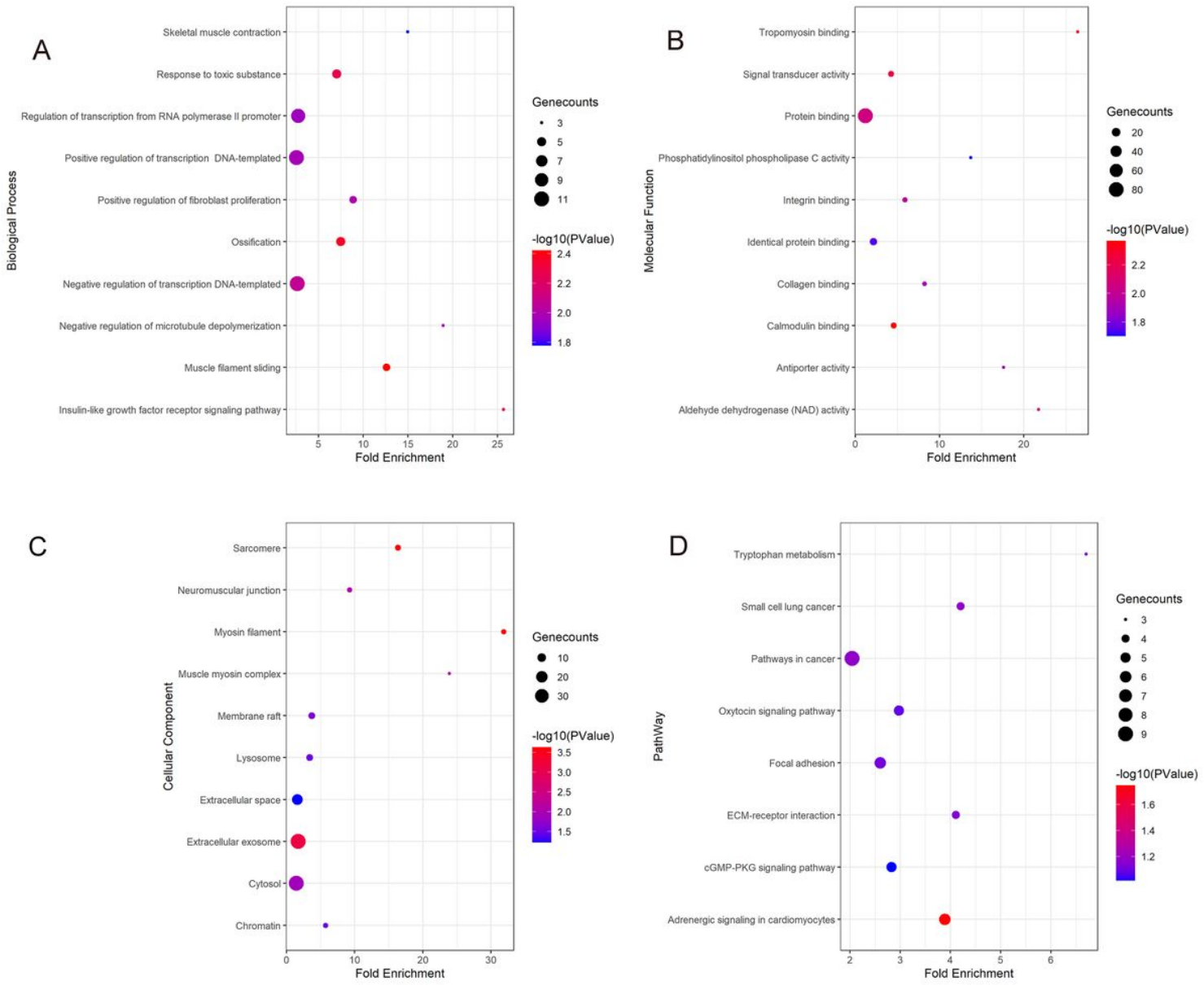

Figure 6

Functional enrichment analyses of overlapping DEGs in IMNM. (A) Biological process term; (B) Molecular function term; (C) Cellular component term; (D) KEGG pathway analysis. Abbreviations: DEGs, differentially expressed genes; KEGG, Kyoto Encyclopedia of Genes and Genomes. IMNM, Immune-mediated necrotizing myopathy.

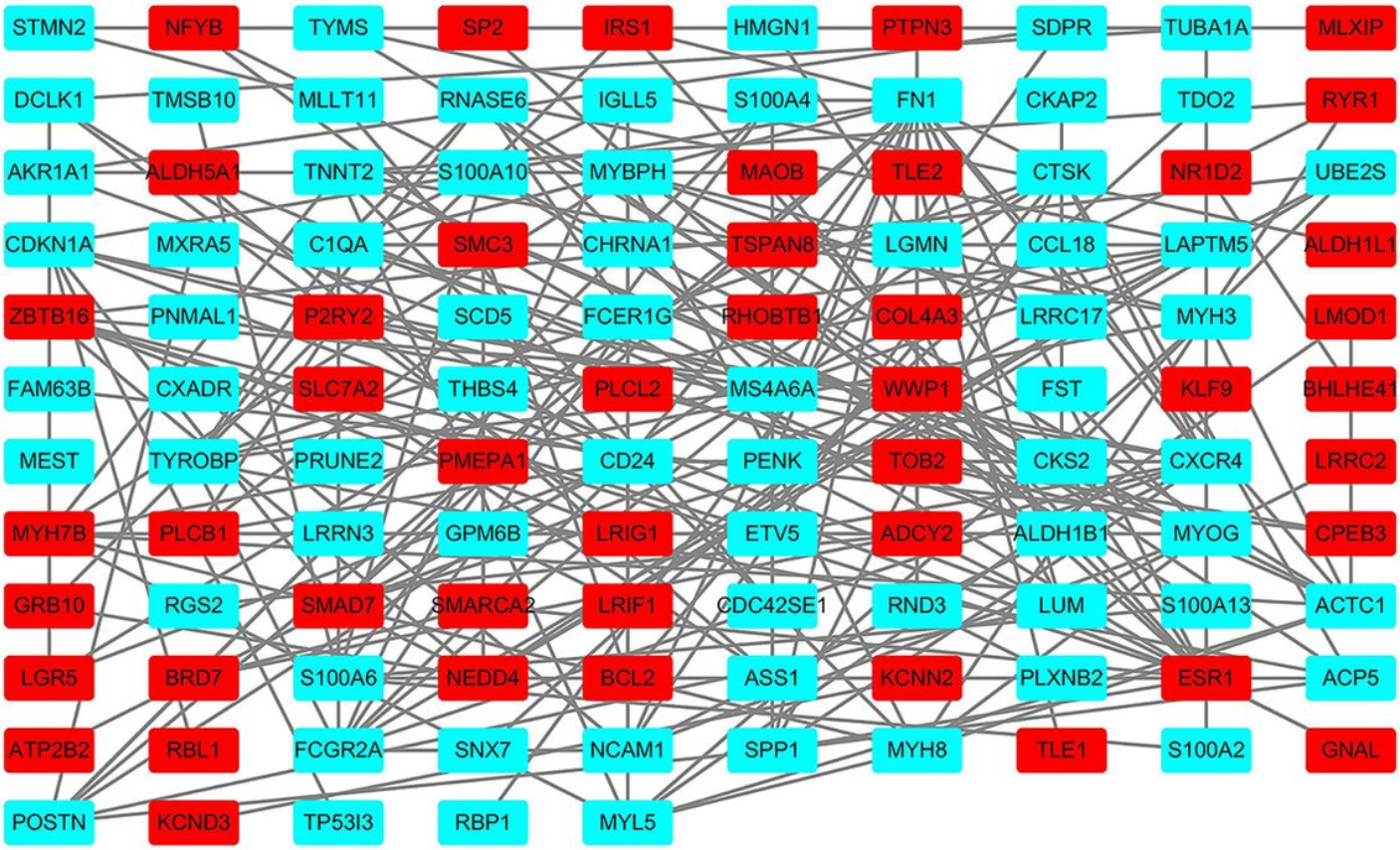

Figure 7

PPI network of the overlapping DEGs. The PPI network consisting of 115 nodes and 205 edges were constructed using STRING database. Each node stands for a gene or a protein, and edges represent the interactions between the nodes. Red nodes represent upregulated genes; blue nodes represent downregulated genes. Abbreviations: PPI, protein-protein interaction; DEGs, differentially expressed genes; STRING, The Search Tool for the Retrieval of Interacting Genes.

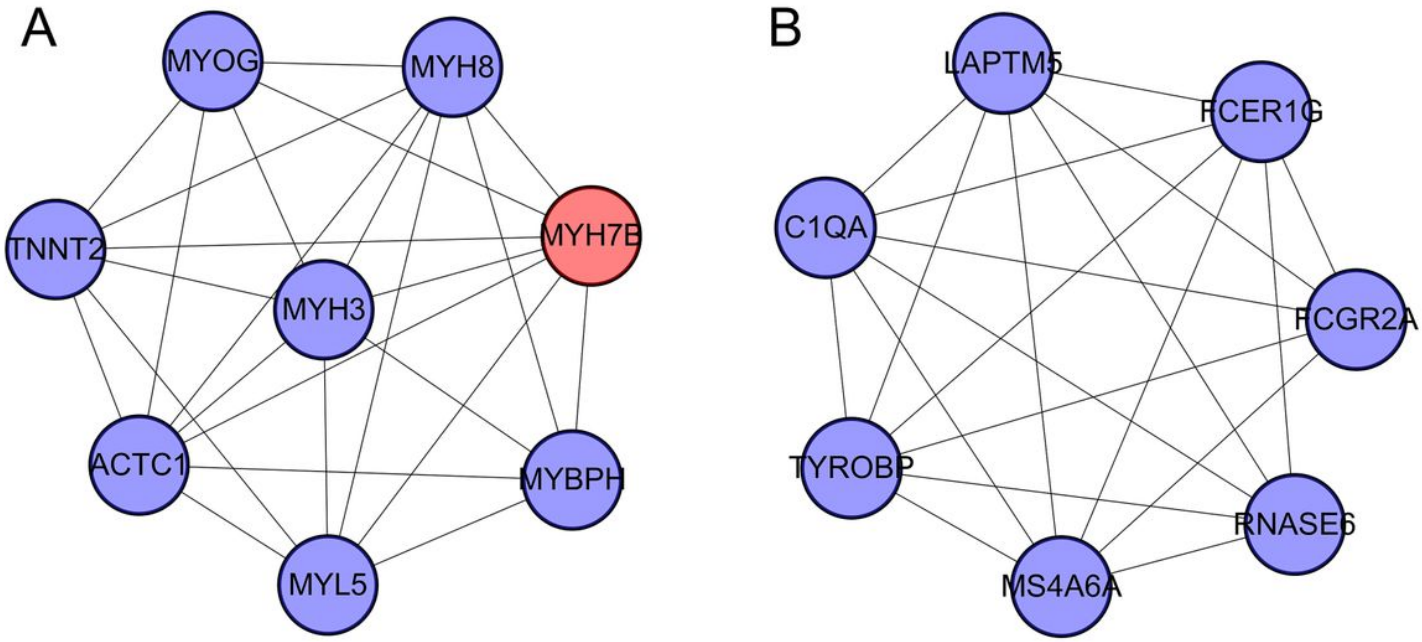

Figure 8

Two significant modules in PPI network selected by MCODE. (A) Module 1; (B) Module 2. Red nodes represent upregulated genes; blue nodes represent downregulated genes. Abbreviations: PPI, protein-protein interaction.

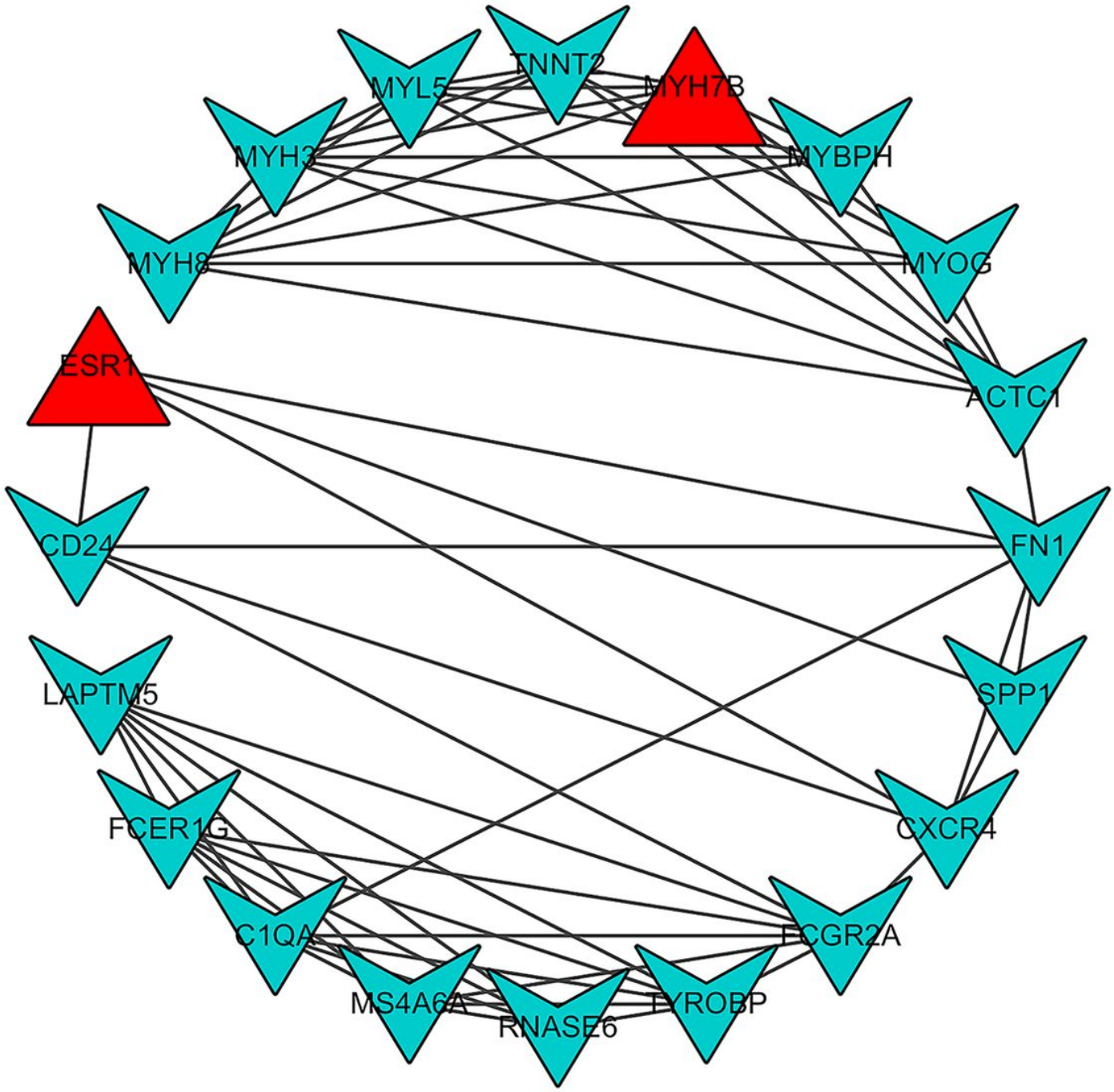

Figure 9

The PPI network of the top 20 hub genes. The shape of triangle represents upregulated genes; the shape of “V” represents downregulated genes. Abbreviations: PPI, protein-protein interaction.